

Seismic and progressive collapse assessment of SidePlate moment connection system

Iman Faridmehr^{*1}, Mohd Hanim Osman¹, Mahmood Bin Md. Tahir¹,
Ali Farokhi Nejad² and Reza Hodjati³

¹UTM-Construction Research Centre, Faculty of Civil Engineering, Universiti Teknologi Malaysia,
Skudai, Johor, 81310, Malaysia

²Faculty of Mechanical Engineering, Universiti Teknologi Malaysia, Skudai, Johor, 81310, Malaysia

³Department of Civil Engineering, Shahrood Branch, Islamic Azad University, Shahrood, Iran

(Received April 21, 2014, Revised November 29, 2014, Accepted September 12, 2014)

Abstract. The performance of a newly generated steel connection known as SidePlateTM moment connection for seismic loading and progressive collapse phenomenon has been investigated in this paper. The seismic evaluation portion of the study included a thorough study on of interstory drift angles and flexural strengths based on 2010 AISC Seismic Provisions while the acceptance criteria provided in UFC 4-023-03 guideline to resist progressive collapse must be satisfied by the rotational capacity of the connections. The results showed that the SidePlate moment connection was capable of attaining adequate rotational capacity and developing full inelastic capacity of the connecting beam. Moreover, the proposed connection demonstrated an exceptional performance for keeping away the plastic hinges from the connection and exceeding interstory drift angle of 0.06 rad with no fracture developments in beam flange groove-welded joints. The test results indicated that this type of connection had strength, stiffness and ductility to be categorized as a rigid, full-strength and ductile connection.

Keywords: sideplate moment connection; interstory drift angle; progressive collapse; seismic performance

1. Introduction

The reliability of established design and construction procedures were truly challenged after the 1994 Northridge, California, earthquake due to development of severe damages in beam-to-column joints that went through rotation levels way below the yield capacity of the framing members.

This unanticipated brittle fracture was against the expected design philosophy of these frames in developing ductile plastic hinges in steel beams that eventually lead to energy dissipation. Hence, significant research activities have been initiated ever since to investigate the behavior of fully restrained connections. At present, the quality acceptance procedure of all moment resisting connections used in special or intermediate steel moment frames is undertaken by using the test protocols designated in Appendix S of the 2010 AISC Seismic Provisions (Specifications 2010).

^{*}Corresponding author, Ph.D. Student, E-mail: s.k.k-co@live.com

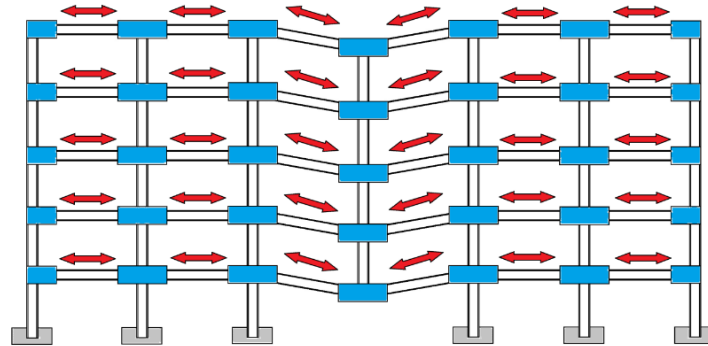


Fig. 1 A typical example of alternate load path

These test protocols endeavor to demonstrate the connection ability to withstand large inelastic deformations through controlled ductile yielding in specific behavioral modes. Apropos the seismic performance of steel moment frames, numerous research programs have been conducted by the Federal Emergency Management Agency “FEMA” (Agency 2002) in the US and also, several reports on seismic design of steel beam column connections including FEMA 350 (Agency 2000) and FEMA 351 (Agency 2000), have been published to facilitate the seismic design process. Prior to the partial collapse of the Ronan Point apartment tower in 1968, engineers were unaware of the significance of structural resistance to progressive collapse. Finally, the 9/11 terrorist attacks triggered the interest in allocation of more funds and budgets to the progressive collapse issue in research projects. Therefore, the alternate load path method for mitigation of progressive collapse phenomenon has been added to a number of design codes including The U.S. General Services Administration, GSA (The U.S. General Services Administration 2003) and Department of Defense, UFC 4-023-03 (Department of Defense 2010). Although local failure is allowed in this approach, provision of alternate load paths within the structure could mitigate the initial damage and consequently, avert the major collapse of the structure. Fig. 1 indicates an example of which an interior column has been removed by blast and the adjacent structural assemblage including beams, columns and joints develop an alternate load path. Redistribution of the applied load on damaged members through catenary action is one of the key mechanisms in mitigation of the spread of “domino” effect. The catenary action is referred to as the ability of beams to resist vertical loads through development of a string-like mechanism (Fig. 1).

The extent of the catenary action is controlled by the beam-column joints as critical elements of any building structure for their limited resistance and rotational capacity. Moreover, a huge spectrum of brittle connection damage has been reported considering the past earthquake observations ranging from minor cracking to completely severed beams and columns. Since the welded flange and bolted or welded web connection (the ‘pre-Northridge’ connection) is not capable of developing sufficient beam ductility in the beam prior to initiation of fracture at the joint, it has become an unacceptable connection to be incorporated in areas of high seismicity. Hence, considerable research has been conducted to mitigate the unexpected damage imposed structures by considering the three following approaches to improve the connection detail:

- i. Improving unreinforced connections /toughening schemes.
- ii. Strengthening approach: strengthening the connection through addition of cover plates, ribs or haunches.

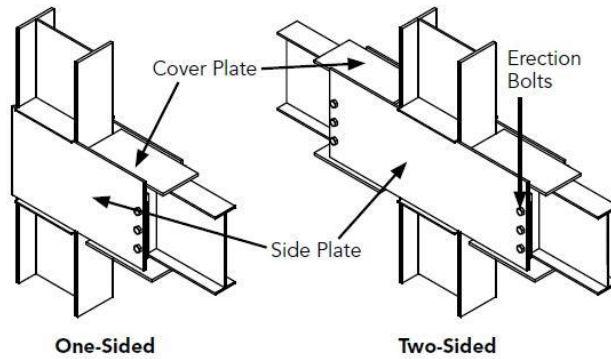


Fig. 2 SidePlate moment connection system

iii. Weakening approach: local weakening of the beam away from the column face by incorporation of reduced beam section (RBS) or slotted web.

Although the original purpose of using SidePlate connections was to meet the seismic demands of structures, an outstanding performance during progressive collapse loading has been demonstrated by such connections which have resulted in extensive application of SidePlate connections in federal buildings of the United States.

In this connection type, a pair of parallel full-depth side plates has been incorporated to join the beam to the column (Fig. 2). Besides, presence of cover plates within the SidePlate connection at beam ends covers the difference among the beam flange width and the wider column flange width. Fillet welding is used to connect the cover plates to the beam flange edges. Meanwhile, a similar detailing for both the cover plate and the column flange width is expected. The peaked triaxial stress concentration existing in all other types of welded moment connections will be eliminated through the physical separation of the beam end and the column. Moreover, application of two thick SidePlates operating with column webs would eliminate the unbalanced shear distortion within the panel zones. The design procedure of the SidePlate connection is composed of considering the following requirements:

- i. Formation of the plastic hinge in the girder or beam should occur at $1/3^{\text{rd}}$ of the girder or beam depth outside the SidePlate end.

- ii. Fabrication of components belonging to all SidePlate connections must be done via application of wide flange or boxed shapes using fillet welds with E70 electrodes.

This study includes an experimental and analytical investigation regarding the progressive collapse and earthquake-resistant capacities of SidePlate moment connection system. For financial limitations facing the full-scale modeling by the authors, the models were scaled down to $1/6^{\text{th}}$ of their real size and were finally set up in the Laboratory of Structures and Materials, Universiti Teknologi Malaysia (UTM), to be compared against the material and geometric nonlinear FEA results obtained from the general purpose FEA software ABAQUS (Hibbitt *et al.* 2001). Interstory drift angles and flexural strengths recommended by 2010 AISC Seismic Provisions (Specifications 2010) were taken into account for seismic assessment whereas the rotational capacities of the connections considering the acceptance criteria provided by UFC 4-023-03 (Department of Defense 2010) guideline were supposed to be satisfied to resist the progressive collapse phenomenon.

2. Previous studies on steel connection behavior

After the World Trade Centre tragedy, the joint integrity was found to be the major parameter in maintaining structural integrity under catenary action and therefore, extensive research work has been conducted ever since. Structural simulations were carried out by Khandelwal and El-Tawil (2007) to study some of the key variables that affect the formation of catenary action in special steel moment-resisting frame sub-assemblages. The sections used in this study were welded joints with and without reduced steel beam sections. Sadek *et al.* (2011) assessed the performance of steel beam-column assemblies with two types of moment-resisting connections both experimentally and analytically analogous to those studied by Khandelwal and El-Tawil (2007) under a middle column-removal scenario. A test program was planned and conducted for a steel frame subjected to blast by Karns *et al.* (2009) in 2009 where both experimental and analytical evaluations were conducted on the behavior of different beam-column joints subjected to blast. Yet, this study is dedicated to the conventional welded moment and side-plate moment connections. To precisely investigate the catenary action development and its influence on the joint behavior, a substructure experimental test along with five beam-column joint tests were conducted by Demonceau (Yang and Tan 2012) where the M-N interaction curves of composite joints, under hogging and sagging moments, were developed in his work. In another study Yang and Tan (2013) experimentally evaluated seven type of bolted steel beam to column connections under the central-column-removal scenario. The study revealed the behaviour and failure modes of different connections as well as their abilities to develop catenary action. At recent research Bo Yang *et al.* (2015) investigated the component-based models of composite beam-column joints under a middle-column-removal scenario. They found component-based models have an acceptable predictions of the composite beam-column joint performance under a middle-column-removal scenario. In case of a sudden column loss as a design scenario, a novel simplified framework for progressive collapse assessment of multi-story buildings were proposed by Izzuddin *et al.* (2009). To successfully validate the rehabilitation performance, three moment connections were rehabilitated by Chou *et al.* (2010) by welding full-depth side plates between the column face and beam flange inner side. Based on results, it was concluded that all rehabilitated moment connections demonstrated excellent performance, where the beam flange tensile strain near the column face were effectively reduced by the presence of the full-depth side plates and exceeding a 4% drift without fractures of beam flange groove-welded joints. The seismic performance of Steel Moment-Resisting Frames (SMRF) with side-plate connections using record-to-record uncertainties were investigated by Jalali *et al.* (2012). An analytical and experimental evaluation of the behavior of WUF-B and SidePlate moment connection geometry during a specified blast event was conducted by Karns *et al.* (2007). According to the results of this study, significantly higher load and rotational capacities were obtained by the SidePlateTM moment connection compared to that of the 'Traditional' WUF-B moment connection configuration, reaching to a limit of 5 times the external energy at first failure. Shao and Hale (2002) conducted an experimental study on three full-scale SidePlate beam to column connections under cyclic loading in accordance with 2002 AISC Seismic Provisions in University of California, San Diego (UCSD). A 992 steel was used for the column and the beam while A572 Grade 50 steel was hired for the plates. It was concluded that two complete cycles of interstory drift angle of 0.04 radians were satisfied by such connections. Also, the results proved the satisfactory performance SidePlate connections to use the full-capacity of connected beam through the formation of the plastic hinge at the beam only.

3. Research methodology and modeling setup

3.1 Case studies and design procedures

Steel Special Moment Frame (SMF) and Intermediate Moment Frame (IMF) systems consist of beam-to-column moment connections prefabricated by SidePlate connection technology. This type of connection lacks direct connections between the beam ends and the columns; instead, two strong full-depth SidePlates are applied to sandwich beam ends to the columns and hence, the anticipated stress concentration at the beam-to-column interface, present in ordinary welded detailing subject to brittle weld fracture, will be eliminated. Moreover, excessive shear distortion of the panel zone will be terminated in this type of connection due to the presence of two thick SidePlates acting in conjunction with column webs. Therefore, the stress concentration due to this high stiffness along with the fracture in weld metal will be terminated eventually. Besides, all applicable requirements of the 2009 IBC (IBC 2009) and 2010 AISC Seismic Provisions (Specifications 2010) are satisfied by the SidePlate moment connection systems.

3.1.1 Lateral bracing of beams

The AISC341-10 Seismic Provisions (Specifications 2010) were considered in provision of the lateral bracing of the beams. The maximum spacing of the lateral bracing of beams are as follows

$$L_b = 0.086 r_y \frac{E}{F_y} \quad (1)$$

Where

r_y = radius of gyration about y axis

E = Modulus of elasticity of steel, E

F_y = Specified minimum yield stress of the type of steel to be used.

3.1.2 Column-beam relationship limitations

Application of Eq. (2) based on the 2010 AISC Seismic Provisions (Specifications 2010) must satisfy the column-beam ratio for SMF systems.

$$\frac{\sum M_{PC}}{\sum M_{Pb}} > 1 \quad (2)$$

Where

$\sum M_{pc}$ is the sum of the projections of the nominal flexural strengths (M_{pc}) of the column above and below the connection joint, at the theoretical hinge formation location in the column. Eq. (3) is used to determine the nominal flexural strength of the column

$$\sum M_{pc} = \sum Z_{ec} \left(F_{yc} - \frac{P_u}{A_g} \right) \quad (3)$$

Where,

Z_{ec} = the equivalent plastic section modulus of the column (Z_c), at a distance of 1/4 of the column depth from the top and bottom edge of the side plates, projected to the beam centerline (in³ or m³).

F_{yc} = the minimum specified yield strength of the column at the connection (psi or Pa).

P_u/A_g = Ratio of column axial compressive load, calculated in conformance with the load and resistance factor provisions, to gross area of the column (psi or Pa).

$\sum M_{pb}$ = The sum of the projections of the anticipated flexural strengths of the beams at the plastic hinge locations to the column centerline. The location of the plastic hinges in the beam must be $1/3^{\text{rd}}$ the beam depth ($db/3$) away from the SidePlate end. The estimated flexural strength of the beam may be determined according to Eq. (4) as follows

$$\sum M_{pb} = \sum (1.1 R_y F_{yb} Z_b + M_v) \quad (4)$$

Where,

R_y = Adjustment coefficient for material over strength, based on Tables 1-6-1 of 2010 AISC Seismic Provisions (Specifications 2010).

F_{yb} = Specified minimum yield strength of the beam.

Z_b = Plastic modulus of the beam section.

M_v = Additional moment caused by shear amplification from the beam hinge location to the column centerline.

The specimens belonged to a five-story structure designed in conformity with AISC-LRFD^{3rd} edition. The original frame along with the case studies configuration is demonstrated in Fig. 3. In addition, Table 1 highlights the beam, column and connection dimensions incorporated in this study. It was assumed that the original frame was a special moment frame having a response modification factor “ R ” of 10 while the design spectral accelerations, namely SDS and SDI , were taken as 2.29 and 0.869 respectively.

3.2 Fabrication and modeling setup

Fabrication of the test specimens was implemented through joint collaboration of commercial fabricators and the university laboratory personnel. The type of welding incorporated in this study was Gas Metal Arc Welding (GMAW). GMAW, frequently referred to as Metal Inert Gas (MIG), welding consists of a group of arc welding processes where powered feed rolls (wire feeder) feed a continuous electrode (the wire) inside the weld pool (Fig. 4). At the beginning of the welding

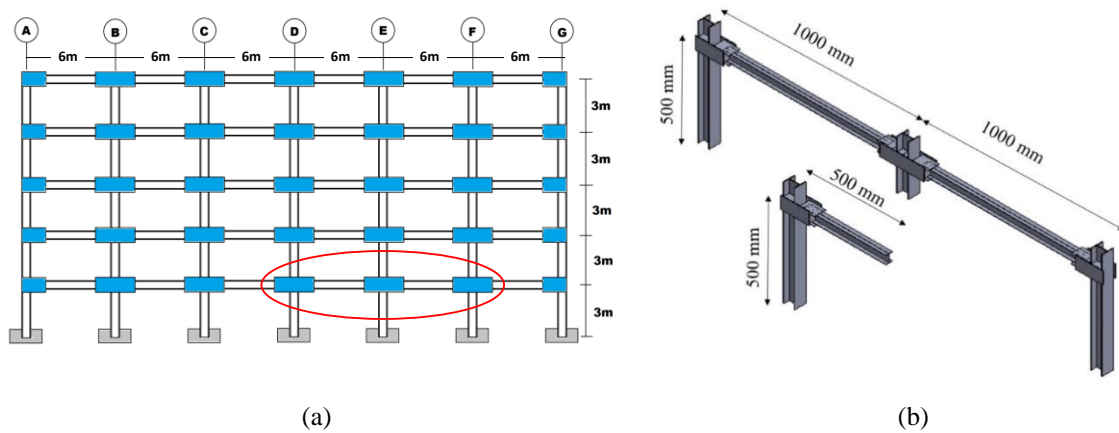
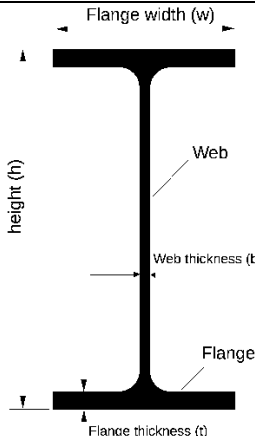
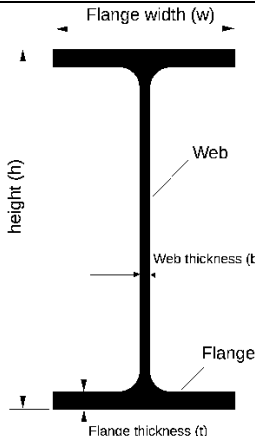


Fig. 3 The original frame (a) Case studies for seismic and progressive collapse assessment (b)

Table 1 Beam, column and connection dimensions selected in this study

Element	Size (mm)		Cross-section (Beam or Column)	Moment of Inertia (mm ⁴)	
	Case Study	Prototype		Case Study	Prototype
Beam Section					
Height (h)	50	360		1040×10 ²	16.27×10 ⁷
Web Thickness (b)	2	8			
Flange Width (w)	40	170			
Flange Thickness (t)	2	12.7			
Column Section					
Height (h)	70	355.6		6900×10 ²	43.7×10 ⁷
Web Thickness (b)	4	17.9			
Flange Width (w)	70	375.9			
Flange Thickness (t)	4	17.9			
Connection Plates					
Center SidePlate	210×75×3	1050×450×12			
Corner SidePlate	140×75×3	700×45×12		-	-
Cover Plate	100×70×2	350×375×10			
Continuity Plate	62×35×2	319.8×200×10			

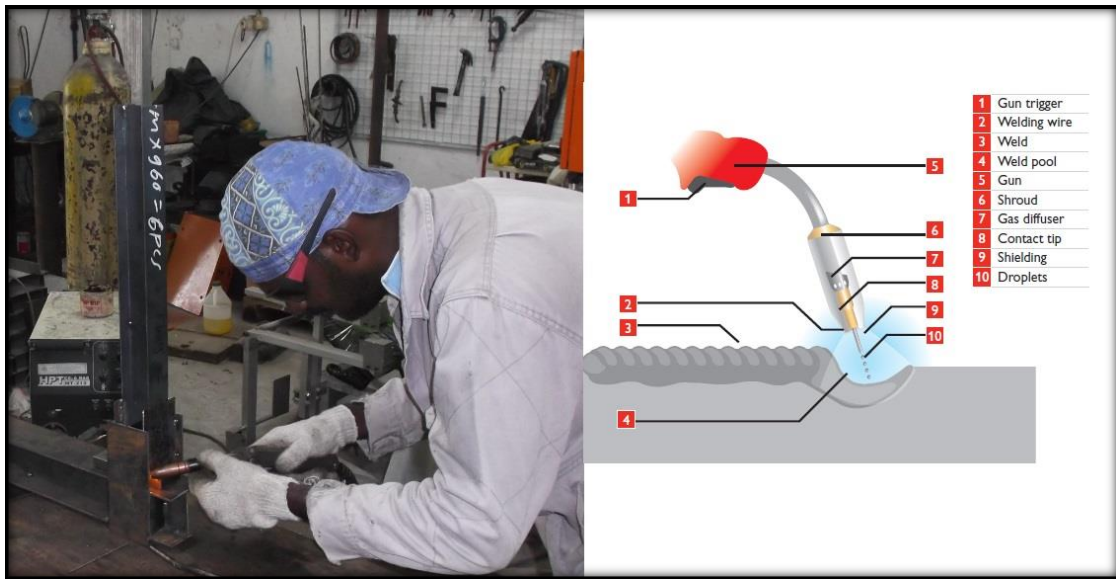


Fig. 4 A schematic view of welding transfer and accessories

process, an electric arc is produced between the weld pool and the tip of the wire. A progressive implementation of wire melting is conducted at the same speed at which it is being fed and therefore, the weld pool is formed accordingly. To effectively protect the arc and the weld pool from atmospheric contamination simultaneously, a nozzle concentric with the welding wire guide tube is applied to deliver a shield of inert (non-reactive) gas for protection purposes. The advantages of this type of welding application are known to be speed, continuity, comparative freedom from distortion and the reliability of automatic welding plus control and versatility of manual welding. The escalating trend of using this technique within mechanized set-ups is

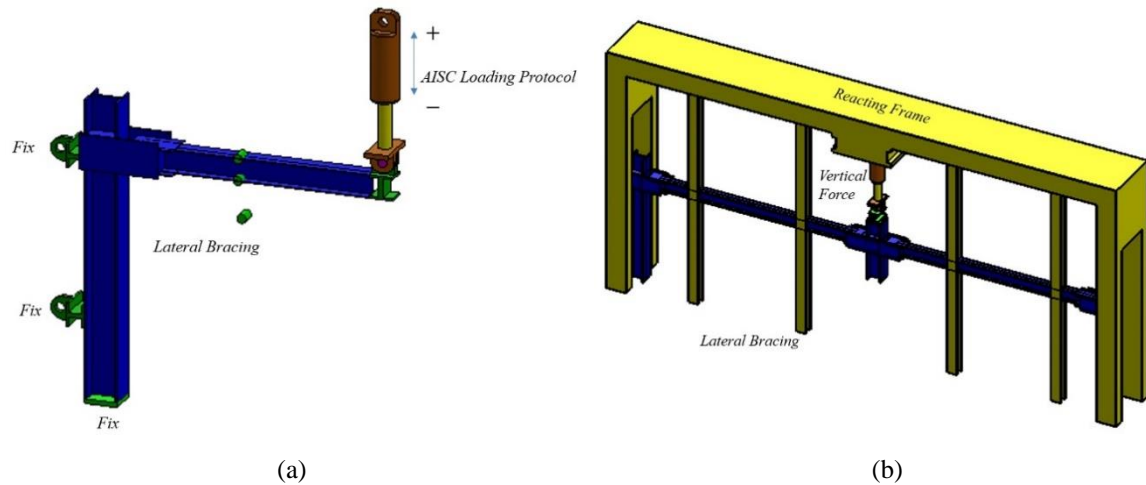


Fig. 5 Modeling set up for seismic (a) and progressive collapse (b) assessment

accelerating. A handheld gun was used to perform *MIG* welding as a semiautomatic process in this project. Speed, voltage, arc (stick-out) length and wire feed rate set to plate thickness are known to be the common welding parameters. Therefore, determination of the filler metal transfer method was accomplished through the arc voltage and wire feed rate. To facilitate the yielding observation within the connection region, the specimens were coated with lime once the welding process was completed.

Different loading protocols and lateral restraint assemblies were selected for the 1/6th scale testing set-ups to assess the seismic and progressive collapse performance of the specimens (Fig. 5). The progressive collapse test of this study was based on the missing column scenario (AP method) where the interior column was considered to be the missing column destroyed by an instantaneous devastating event. Simulation of the quasi static loading adopted for this test was achieved through application of a monotonically increasing “ramp” (Fig. 6). Both sides of the beams were laterally restrained at locations 150 and 800 mm from the centerline of the specimen column. To successfully conduct and evaluate the cyclic test of the seismic specimens, a hydraulic actuator to the tip of the beam was hired. The Hydraulic pseudo-dynamic actuator incorporated in this study has a capacity of 250 kN for both compression and tension along with a 500-mm maximum piston stroke (Fig. 6). It is good to mention that both sides of the beams were laterally restrained at middling length of beam from the centerline of the specimen column. The internal force measurements were conducted by placing a number of strain gauges at predictive hinge locations of steel beams, usually at beam ends. To precisely measure the vertical deflection of the specimen, Linear Variable Differential Transducers (*LVDTs*) were placed at location of removed column and tip of the beam to assess the progressive collapse and seismic performance respectively. Other assumptions considered in this study are as follows:

- i. The tests were two-dimensional only and specimens were constrained in plane. The influence of out-of-plane beams concurring to the joint was ignored.
- ii. Slab effects were ignored (“conservative” approach).
- iii. Zero stresses resulting from gravity and live loads plus zero velocity were assumed to be the initial conditions of the specimens.

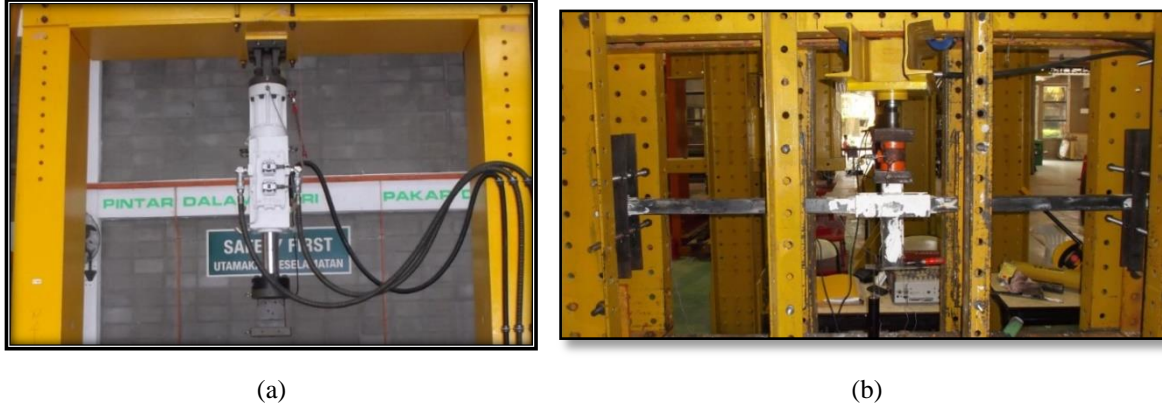


Fig. 6 The dynamic actuator (a) and hydraulic jack (b) used for seismic and progressive collapse evaluation

Table 2 Scale factors for conversion scale-down model to full-scale

Quantities	Symbol	Scale Factor Value
Material-Related Properties		
Modulus of Elasticity	S_E	1
Strain	S_ϵ	1
Stress	S_σ	1
Poisson's Ratio	ν	1

Scale model fabrication is concerned with the replication of prototype geometry and all details that may significantly influence the structural behavior. However, the specific characteristics of steel structures are easier to simulate than others where for some materials will be almost impossible to replicate at small scales. Generally, design and fabrication scale model of steel structures, phenomenon such as initiation and propagation of yielding, buckling of elements and lateral torsional buckling can be properly simulated. On the other hand, scaling procedure in the connections is a difficult task. For example at welded beam to column connections where in small-scale models welds will be oversized, it would be inappropriate to study such localized characteristics as weld fracture or column flange distortion. As already mentioned, in this research gas metal arc welding “MIG” was employed as it possible in this method to calibrate the size of groove welding with base metal.

Conversion of a scaled-down model to a full-scale one is achieved by using the fundamental scaling factors including, the scaling factor for the material elastic modulus, S_E , the scaling factor for strain, S_ϵ and the scaling factor for stress, S_σ . Since the prototype and scale-model are both made of the same steel material, then $S_E = S_\epsilon = 1$. To compute the above mentioned scaling factors, the following equations will be used that summarized in Table 2.

$$S_E = \frac{\text{Prototype Model}}{\text{Scale Model}} = 1 \quad (5)$$

$$S_\epsilon = \frac{S_{\Delta L}}{S_L} = 1 \quad (6)$$

$$S_{\sigma}=S_E S_{\varepsilon}=1 \quad (7)$$

3.3 Finite element modeling procedure and material properties

The *FE* software *ABAQUS/STANDARD* (Karlsson *et al.* 2001) was used to execute the *FEA* phase of the study because it was appropriate to model large deformations and strains. To obtain a better response from the software model, the eight-node solid *C3D8R* element having six degrees of freedom representing three force components and three moment components simultaneously has been used. To achieve a mesh of finer size in the connection area, the hex element was incorporated in all *FE* models. To appropriately model the material behavior, the true stress-strain curve has been incorporated (Faridmehr *et al.* 2014). Displacements and strains are introduced by the following formulas for a *FEA* representation

$$e = \frac{\Delta l}{l} \quad (8)$$

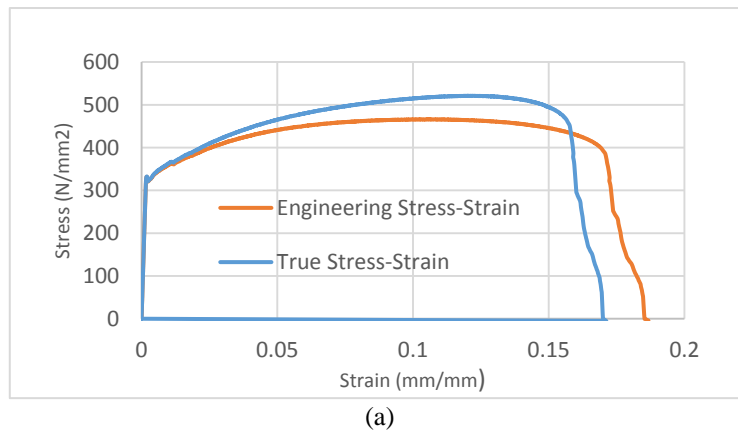
$$S = \frac{P}{A_0} \quad (9)$$

$$\sigma = s(1+e) \quad (10)$$

$$\varepsilon = \ln(1+e) \quad (11)$$

Where; e and S are engineering strain and stress respectively determined from the uniaxial tensile test and subsequently, σ and ε as the true stress and strain will be computed from Eqs. (10) and (11) respectively. Fig. 7 indicates the true and engineering stress-strain curves plus the universal testing machine hired to conduct the tests.

The yield stress and ultimate tensile strength values after the conduction of tensile testing were 320 MPa and 510 MPa respectively. In all cases of the *FEA*, application of load was performed by



(b)

Fig. 7 Material properties for true stress-strain and engineering stress-strain (a), universal testing machine (b)

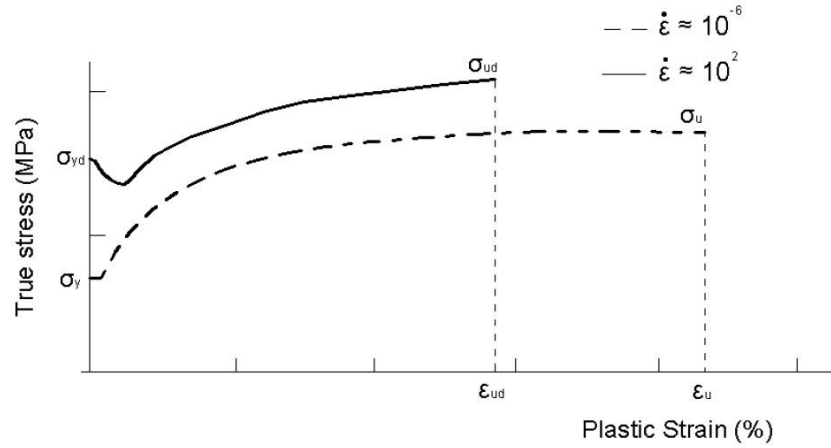


Fig. 8 Monotonic flow curve for low and high strain rates

Table 3 Dynamic increase factors (DIFs) for low-pressure explosions

Material	Yield Stress		Ultimate Stress
	Bending/Shear	Tension/ Compression	
A36	1.29	1.19	1.10
A588	1.19	1.12	1.05
A514	1.09	1.05	1.00
A446	1.10	1.10	1.00

displacement control in vertical direction in addition to fixing the column base in all degrees of freedom. A quasi static loading rate of 2 mm/s and 0.5 mm/s was selected for progressive collapse and cyclic loading respectively.

Extreme events like vehicle impact, gas explosions and terrorist suicide attacks are listed as strong dynamic processes entailing high strain rates. Consequently, high strain rates result from the global response of parts or the entire structure that have dynamic effects along with strain rate effects within the material response. A different response is anticipated from steel material under high loading rates compared to static loading conditions that proves the dependence of stress-strain relationship on strain rates. The following is a summary of the main features of this behavior (Fig. 8):

- The Yong's modulus is unaffected.
- The ultimate tensile strength rises slightly with strain rate.
- A much higher increase is demonstrated by the yield strength, in comparison.
- The ultimate tensile strain is able to reduce with strain rate.

Application of dynamic increase factors (DIFs) to describe strain rate enhancement has been proven to be useful. Such factor is incorporated to modify the static stress resulting from dynamic loadings and it is defined to design blast resistant structures in conformity with UFC 3-340-02 (UFC 2014). The DIF values for standard steel, as a common structural material within the US, are based on the average strain ratio of 0.1 in/in/sec, which is an indication of low-pressure explosions. Higher strain ratio values will result in higher values of DIF. Also, DIF values of different average strain rates have been provided in UFC 3-340-02 (UFC 2014).

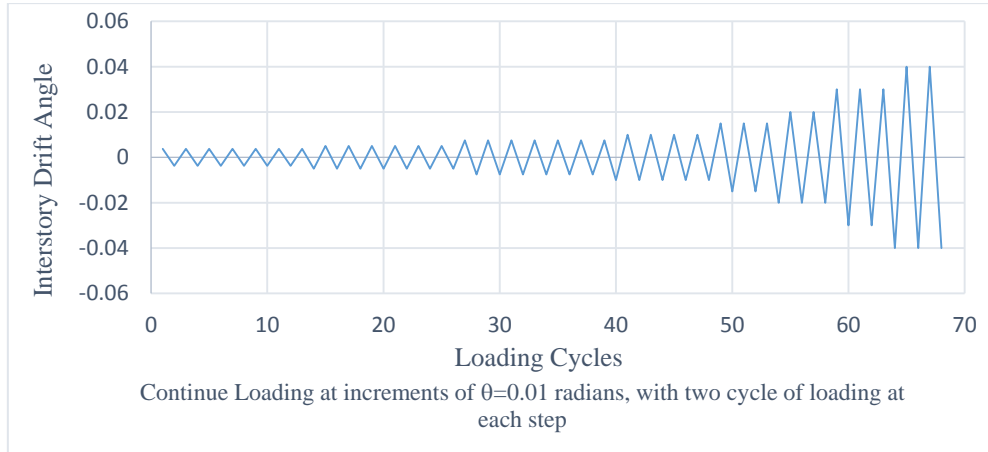


Fig. 9 The loading protocol used for seismic assessment

Hence, it would be better to conduct impact condition tests of which the structures are under (a) deformations at a moderately low temperature, (b) a high strain rate (i.e., deformation rate), and finally (c) a triaxial stress condition that could be provided through the use of a notch to successfully seize the precise mechanical properties of a material. The Charpy impact test aka the Charpy V-notch test is aimed at determination of the energy absorbance of a material during fracture (Toshiro *et al.* 1986, Rossoll *et al.* 2002, Tanguy *et al.* 2005). Such absorbed energy indicates the notch toughness of a given material and is used as a tool to investigate the temperature-dependent ductile-brittle transition. Since the quasi-static loading was chosen for both the cyclic and progressive collapse loading of this study, the steel properties sensitivity to high strain rate was neglected.

3.4 Loading protocol

The 2010 AISC Seismic Provisions (Specifications 2010) were taken into account in seismic evaluation of the loading sequence employed in this study. Fig. 9 shows a series of load steps and the number of cycles required for each one as indicated in AISC Protocol. Each total inter story-drift angle is related to a particular load step. The testing procedure started with application of load steps plus recording the data points at regular intervals. Once each load step was completed, photographs were taken and observations were recorded accordingly. By the time the strength of the specimen reduced to 40 percent of the maximum strength, the loading was stopped. To properly assess the progressive collapse phenomenon, the vertical push-down analysis was carried out through gradually increasing the vertical displacement at the removed column location to study the connection rotational capacity and resistance of the structure against such deformation.

3.5 Acceptance criteria based on AISC 341-10 and UFC 4-023-03

In the design of the *SMF* in conformance with the 2010 AISC Seismic Provisions (Specifications 2010), providing substantial inelastic drift capacity by flexural yielding of the *SMF* beams and limited yielding of column panel zones must be considered. Besides, a stronger design for the columns must be considered compared to those of fully yielded and strain-hardened beams

or girders. Finally, the following seismic requirements for beam-to-column connections must be satisfied:

- i. The connection must sustain an inter story drift angle of at least 0.04 rad (Fig. 10(a)).
- ii. The flexural resistance of the connection determined at the column face must be equal to at least 0.80 Mp of the connected beam at an inter story drift angle of 0.04 rad.

Provision of adequate connection rotational capacity is a prerequisite for arresting progressive collapse (Fig. 10(b)). Despite the fact that moment connections are prequalified for rotational capacity due to bending alone, they fail to concurrently resist the interaction of axial tension and bending moment that is the prevailing problem in progressive collapse. Although the load carrying capacity of the system against bending moment alone could greatly be increased by tension stiffness ('cable-like' action), the combination of bending moment and axial tension develop large flange tension forces that must be transferred by the beam-to-column connection. Table 5-2 of UFC 4-023-03 (Department of Defense 2010) highlights the design strength and rotational capacities of the beam-to-column connections used in progressive collapse assessment (Table 4).

4. Results and discussion

4.1 Progressive collapse assessment

The typical behavior of the double-span beams according to FEA and experimental results are presented in this section. The key variable in progressive collapse assessment is plastic rotation

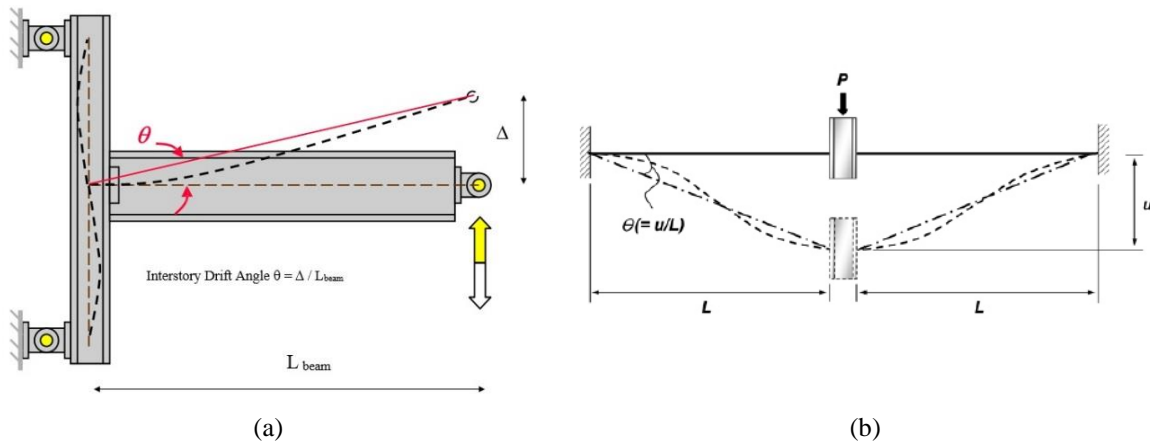


Fig. 10 Definition of interstory drift angle (a) and plastic hinge rotation angle (b)

Table 4 Acceptance criteria for progressive collapse assessment

Connection Type	Plastic Rotation Angle (θ), radians	
	Primary	Secondary
SidePlate TM	0.089-0.0005d	0.169-0.0001d
<i>d = depth of beam, inch</i>		

angle (θ) defined as the vertical deflection of the column (u) divided by the clear span length of the beam (L) (Fig. 10(b)).

According to the data collected by photographic documentation, direct observation and data logger, it was revealed that at first stage of failure, plastic hinges initiated at the quarter beam depth from the end of the SidePlate at a vertical load of 6.5 kN. At this stage, the beam flanges experienced a slight but visible buckling. Formation of plastic hinges was verified at a yielding level above $1800 \mu\epsilon$ (micro-strain) recorded by a strain gauge. Then, at later stages of the push-down, the quarter beam depth from the end of the SidePlate exhibited full formation of the expected plastic mechanism. However, observation of significant global hardening was the noticeable fact. This issue confirms the ability of the SidePlate to develop the full capacity of connected beams. Furthermore, once the vertical loading was in the range of 10 to 15 kN, most of the strain gauges were well beyond yield level and showed recorded strains of $5000 \mu\epsilon$ (i.e., almost 3 times above the yield level). At a vertical load of 19 kN and a plastic hinge rotation angle of around 0.2 rad, beam flanges experienced a series of fractures and at this stage, the progressive collapse phenomenon caused the degradation and demise of the SidePlate specimen. By the time the SidePlate moment connection reached to large vertical displacements, development of catenary action resulting from the good performance of the SidePlate moment connection is noticeable. The following failure modes are listed for the SidePlate: (i) plastic rotation of members (plastic hinges), (ii) inelastic local buckling of web or flange of steel sections for beams, where in some extreme cases ended up as fractures, (iii) fracture initiation at the flange at the tension side of the beam with further propagation to the web. The damaged state of the specimen in addition to the plastic equivalent strain distribution after the final stage of progressive collapse test is shown in Fig. 11.

The analytical and experimental visualized plots of the SidePlate specimen in terms of vertical load versus the plastic hinge rotation angle of the progressive collapse tests are shown in Fig. 12. According to the recorded data, a good agreement exists among the experimental and analytical results of the tests in terms of yield point, strain hardening, modes of failure and maximum plastic

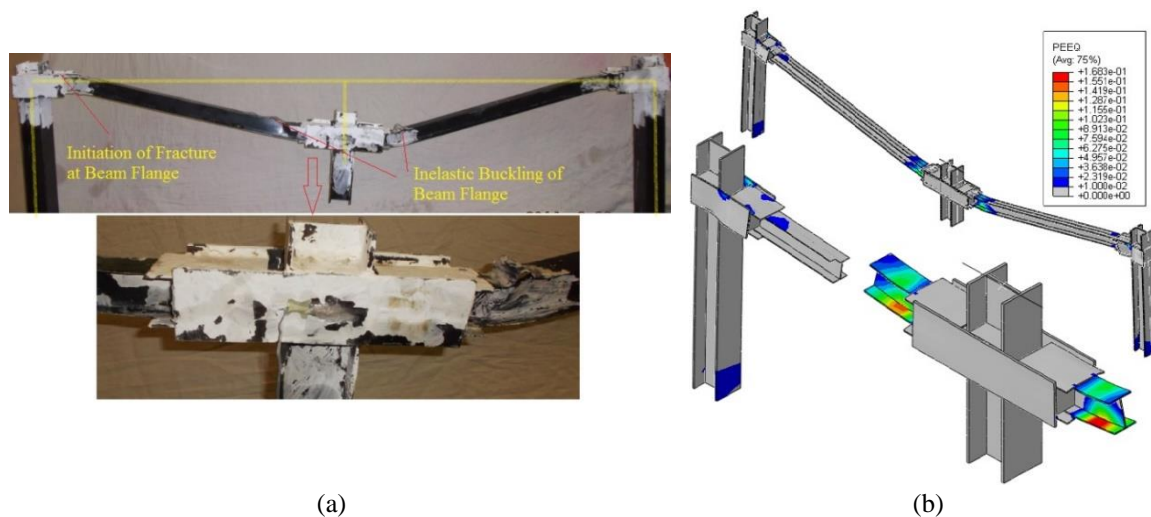


Fig. 11 Damaged state of the specimens after the end of progressive collapse test (a) and plastic equivalent strain distribution (b)

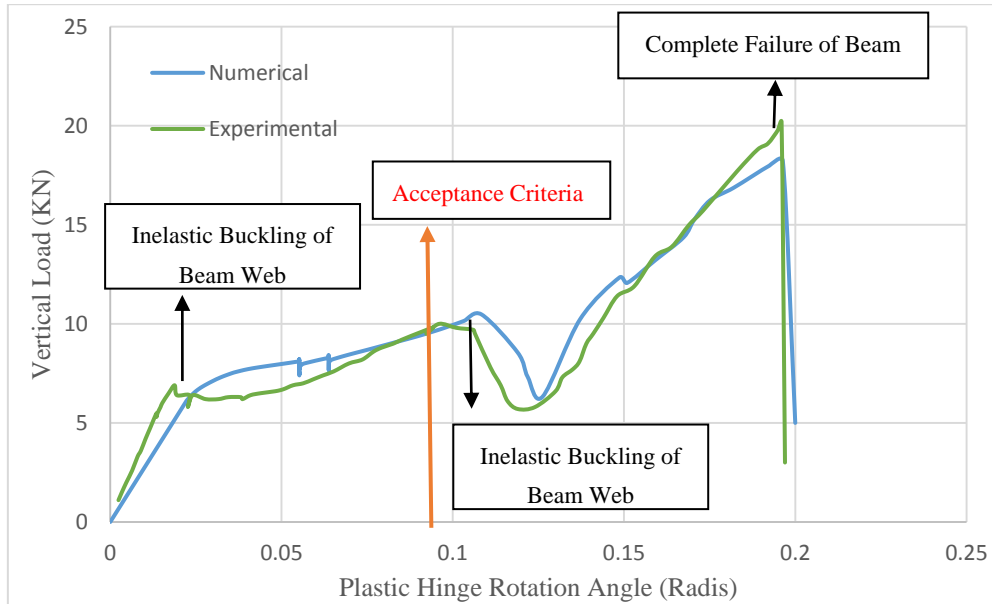


Fig. 12 Force vs. plastic hinge rotation angle for progressive collapse tests

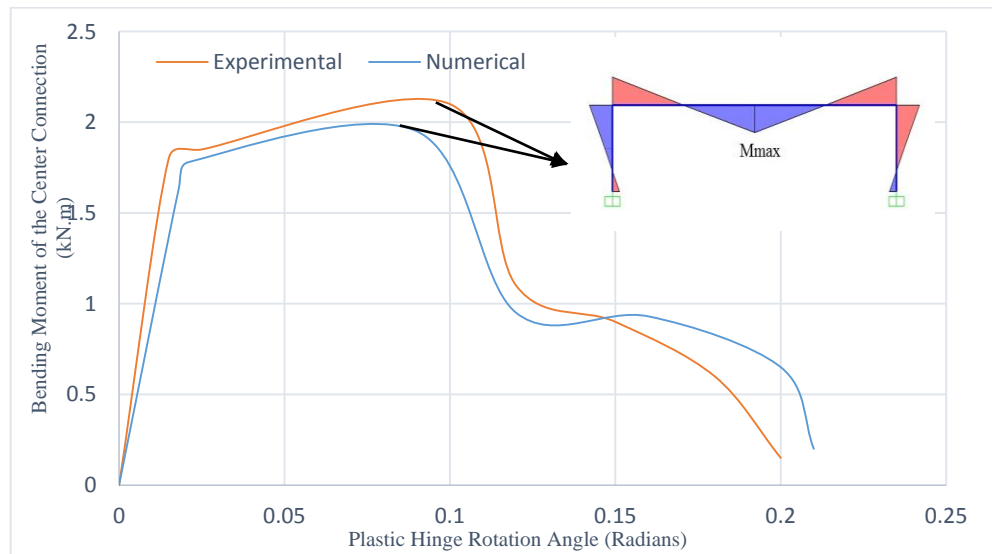


Fig. 13 Bending moment vs. plastic hinge rotation angle for progressive collapse tests

hinge rotations.

Fig. 13 depict the bending moment of the center connection versus plastic hinge rotation angle. The maximum moment appeared in the two side of removed column which in experimental test the beam experienced moment around 1.2 times bigger than plastic moment (M_p).

Table 5 shows a comparison between the recorded experimental and analytical results of the progressive collapse performance of the SidePlate specimen used in this study.

Table 5 Result summaries of progressive collapse evaluation

Moment Connection Type	Vertical Force at First Fracture (KN)		Max Vertical Force at End of Test (KN)		Joint Rotation at First Fracture (Radians)		Joint Rotation at End of the Test (Radians)		Mode of Failure	
	Analysis	Test	Analysis	Test	Analysis	Test	Analysis	Test	Analysis	Test
SidePlate	10.4	10	18.2	20.2	0.11	0.1	0.19	0.19	Beam Failure	Beam Failure

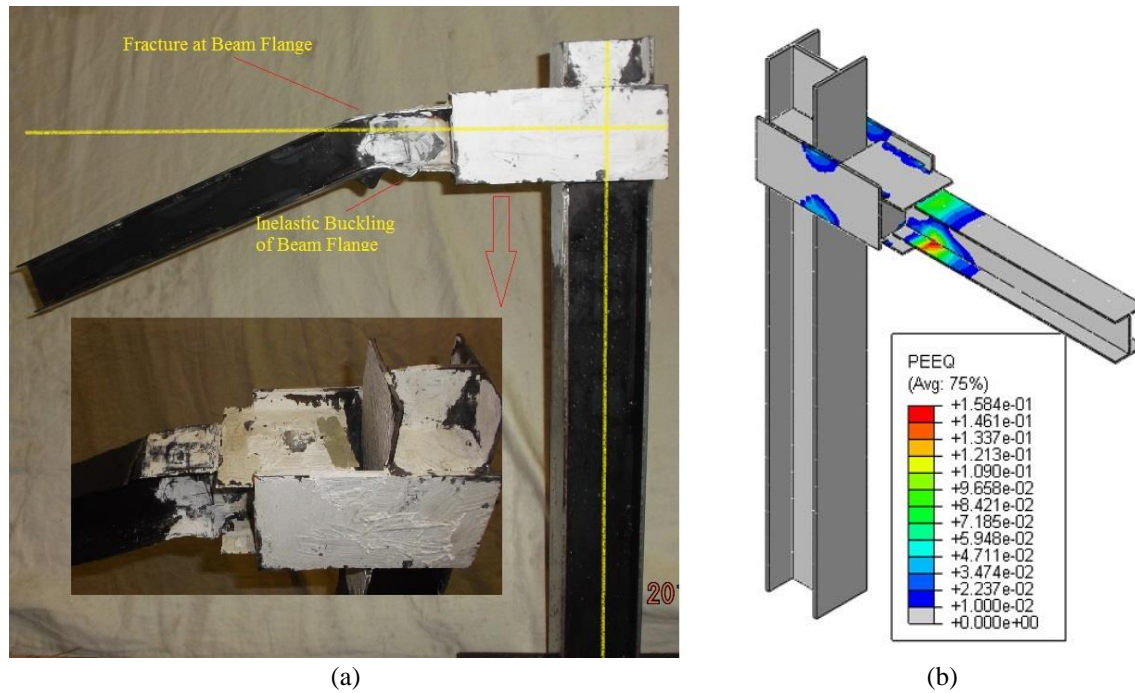


Fig. 14 Damaged state at the end of seismic test (a) and plastic equivalent strain distribution (b)

4.2 Seismic assessment

The seismic performance of the SidePlate Connection Specimen will be discussed in this section. Interstory drift angle is considered to be the fundamental parameter in assessing the seismic performance of structures (Fig. 10(a)). Observation of minor flaking of the whitewash coating at the top beam flange region is the first sign of yielding occurrence at the SidePlate Connection Specimen during the first cycle of 0.015 story drift cycles. Although, the entire beam flange demonstrated signs of yielding during the 0.03 story drift, no signs of yielding were observed in the SidePlates and the beam cover plates at the same story drift value. Yet, this interstory drift angle maintained the peak strength. Besides, the groove weld between the shear plate and column face went through a minor fracture at an interstory drift angle of 0.05 rad. The inelastic buckling of the beam top flange caused a slight decrease in strength towards the interstory drift angle of -0.05 rad. This top flange buckling was prior to the beam web buckling despite its very small amplitudes. Next, the groove welding between beam top flange and beam web

indicated a few cracks at an interstory drift angle of 0.06. After that, low cycle fatigue cracks were initiated in the base metal at this location. Last but not least, more extensive cracks were initiated as they extended down into the web plate during the first cycle of 0.07 story drift. Extensive plastic deformation and energy absorption “toughness” before developing fracture in the base metal was observed. Notice that, Fatigue failure proceeds in three distinct stages: (i) crack initiation in the areas of stress concentration (near stress raisers), (ii) incremental crack propagation and (iii) final catastrophic failure. Despite the fact that no column or panel zone yielding occurred during the test, one complete cycle of an interstory drift angle of 0.07 was resisted by the SidePlate Connection Specimen. Finally, appearance of fractures in the web and in the top flange of the beam was an indication of termination of the test. At final stage of the test, the strain gauges placed on beam flanges showed records beyond $4800 \mu\epsilon$ (micro-strain) indicating the development of fully plastic capacity of connecting beams. The experimental failure mode and the plastic equivalent strain distribution at the end of cyclic test are shown in Fig. 14.

The computed moment at the column face versus interstory drift angle recognized as the global seismic response of the SidePlate connection specimen is shown in Fig. 15. The results of the theoretical model and the experimental test were in good agreement in the overall cyclic behavior. Besides, numerical results also confirmed the formation of plastic hinges at the beam flange. To simulate of failure behavior, the ductile damage as constitutive equation was applied. Therefore, the fracture strain was used according to displacement criteria which in this research the fracture strain was 0.16 mm/mm. No degradation signs were observed in the hysteretic responses of the SidePlate connection specimen during the FEA. Still, a decrease in the hardening slope in addition to a flattening of the curve during the last cycles were resulted from the local buckling initiation of the beam flange at an interstory drift angle of 0.06. All in all, a good agreement was observed in yielding and buckling patterns of the analytical model and experimental test results.

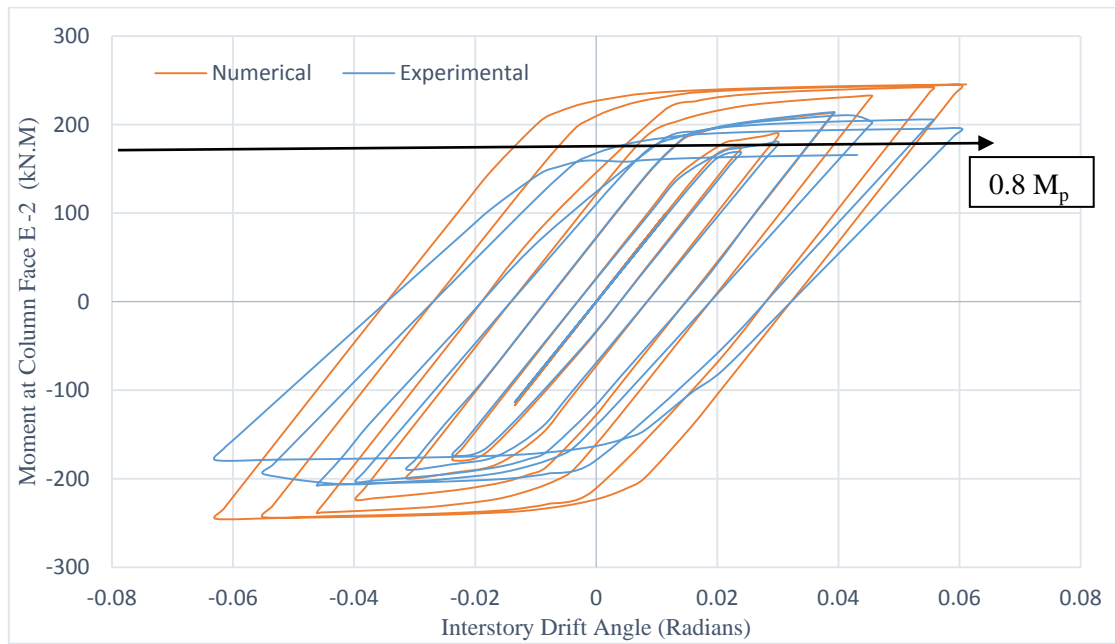


Fig. 15 Moment at column face versus interstory drift angle

Table 6 Result summaries of seismic evaluation

Moment Connection Type	M/M_p First Fracture		M/M_p Maximum		Interstory Drift Angle at First Fracture (Radians)		Interstory Drift Angle at End of the Test (Radians)		Mode of Failure	
	Analysis	Test	Analysis	Test	Analysis	Test	Analysis	Test	Analysis	Test
SidePlate	1.13	1.01	1.225	1.07	0.05	0.04	0.07	0.06	Beam Failure	Beam Failure

Table 6 presents a comparison between the recorded experimental (test) and analytical (analysis) results of seismic evaluation for the SidePlateTM moment connection used in this study.

5. Conclusions

The seismic and progressive collapse performance of the SidePlate moment connection system was investigated in this study. The interstory drift angle and flexural strength conforming to 2010 AISC Seismic Provisions (Specifications 2010) in addition to plastic rotation angle conforming to UFC 4-023-03 (Department of Defense 2010) guideline were the fundamental acceptance criteria for seismic and progressive collapse evaluation in this project respectively. The following conclusions have been drawn based on the experimental and analytical test results:

- i. The SidePlate moment connection was capable of achieving adequate rotational capacity, developing catenary action and also developing the full inelastic capacity of the connecting beam.
- ii. The SidePlate moment connection system achieved significantly high load and rotational capacities in progressive collapse test reaching 3 times the external energy at first failure.
- iii. Precise progressive collapse evaluations indicated that the failure mode and the formation of catenary action were controlled by the tensile capacities of beam-column joint after undergoing large rotations. This implies that high tensile resistances of beam-column joints after undergoing large rotations should be adopted by engineers than pure tying resistance. If large rotations are ignored in the design stage, the joints having poor rotation capacities will not be able to achieve the design tying resistances.
- iv. According to seismic performance result tests, one complete cycle of an interstory drift angle of 0.07 was satisfied by the SidePlate moment connection system. Therefore, this connection indicates a very good performance in case of a terrorist bomb blast including progressive collapse and seismic force.
- v. The maximum moment developed at a quarter of beam depth from the end of the side plate was almost 1.20 times bigger than the actual beam plastic moment, M_p . Also, the strain hardening value of 1.5 calculated according to FEMA 350 (Agency 2000) was exceeded during the experimental tests.
- vi. There is a need to account for rate sensitivity in a progressive collapse scenario where component ductility may be drastically reduced due to steel ultimate strain rate sensitivity. Accordingly, it suggested to run experimental test with sudden removal column to take into account rate sensitivity.

Acknowledgements

The authors wish to thank the esteemed technical staff of the Laboratory of Structures and Materials, Universiti Teknologi Malaysia (UTM) for their cooperation and support in this study. The financial support provided by the University for conducting the experimental work is also appreciated.

References

- Agency, F.E.M. (2000), Recommended Seismic Design Criteria for New Steel Moment-Frame Buildings "FEMA 350", U. D. o. H. Security, United States of America.
- Agency, F.E.M. (2002), Federal Emergency Management Agency, U. D. o. H. Security, United States of America.
- Chou, C.C., Tsai, K.C., Wang, Y.Y. and Jao, C.K. (2010), "Seismic rehabilitation performance of steel side plate moment connections", *Earthq. Eng. Struct. Dyn.*, **39**(1), 23-44.
- Department of Defense (2010), Design of Buildings to Resist Progressive Collapse, UFC 4-023-03.
- Dihong Shao, T.H. (2002), *Full Scale Testing and Project Application of SidePlate™ Moment Connection for SMRF Using Deep Columns*, California, Office of Statewide Health Planning and Development Sacramento.
- Faridmehr, I., Osman, M.H., Adnan, A.B., Nejad, A.F., Hodjati, R. and Azimi, M.A. (2014), "Correlation between engineering stress-strain and true stress-strain curve", *Am. J. Civil Eng. Arch.*, **2**(1), 53-59.
- IBC, I. (2009), International building code, International Code Council, Inc. (formerly BOCA, ICBO and SBCCI) 4051, 60478-65795.
- Jalali, S., Banazadeh, M., Abolmaali, A. and Tafakori, E. (2012), "Probabilistic seismic demand assessment of steel moment frames with side-plate connections", *Scientia Iranica*, **19**(1), 27-40.
- Karlsson, H. and Sorensen (2001), ABAQUS/Standard user's manual, Hibbitt, Karlsson & Sorensen.
- Karns, J.E., Houghton, D.L., Hall, B.E., Kim, J. and Lee, K. (2007), "Analytical verification of blast testing of steel frame moment connection assemblies", *Proceedings of the Research Frontiers Sessions of the 2007 Structures Congress*.
- Karns, J.E., Houghton, D.L., Hong, J.K. and Kim, J. (2009), "Behaviour of varied steel frame connection types subjected to air blast, debris impact, and/or post-blast progressive collapse load conditions", Austin, TX, United States, 1868-1877.
- Khandelwal, K. and El-Tawil, S. (2007), "Collapse behavior of steel special moment resisting frame connections", *J. Struct. Eng.*, **133**(5), 646-655.
- Rossoll, A., Berdin, C. and Prioul, C. (2002), "Determination of the fracture toughness of a low alloy steel by the instrumented Charpy impact test", *Int. J. Fract.*, **115**(3), 205-226.
- Sadek, F., Main, J.A., Lew, H. and Bao, Y. (2011), "Testing and analysis of steel and concrete beam-column assemblies under a column removal scenario", *J. Struct. Eng.*, **137**(9), 881-892.
- Specifications, A. C. o. (2010), Seismic Provisions for Structural Steel Buildings "ANSI/AISC 341-02", American Institute of Steel Construction, Inc.
- Tanguy, B., Besson, J., Piques, R. and Pineau, A. (2005), "Ductile to brittle transition of an A508 steel characterized by Charpy impact test: Part I: experimental results", *Eng. Fract. Mech.*, **72**(1), 49-72.
- The U.S. General Services Administration (2003), Progressive Collapse Design Guidelines Applied to Concrete Moment-Resisting Frame Buildings. Washington (DC).
- Toshiro, K., Isamu, Y. and Mitsuo, N. (1986), "Evaluation of dynamic fracture toughness parameters by instrumented Charpy impact test", *Eng. Fract. Mech.*, **24**(5), 773-782.
- UFC (2014), Structures to resist the effects of accidental explosions "UFC 3-340-02", Unified Facilities Criteria (UFC).
- Vlassis, A., Izzuddin, B., Elghazouli, A. and Nethercot, D. (2009), "Progressive collapse of multi-storey

- buildings due to failed floor impact”, *Eng. Struct.*, **31**(7), 1522-1534.
- Yang, B. and Tan, K.H. (2012), “Numerical analyses of steel beam-column joints subjected to catenary action”, *J. Construct. Steel Res.*, **70**, 1-11.
- Yang, B. and Tan, K.H. (2013), “Experimental tests of different types of bolted steel beam-column joints under a central-column-removal scenario”, *Eng. Struct.*, **54**, 112-130.
- Yang, B., Tan, K.H. and Xiong, G. (2015), “Behaviour of composite beam-column joints under a middle-column-removal scenario: Component-based modelling”, *J. Construct. Steel Res.*, **104**, 137-154.

CC